RSC Advances

PAPER

View Article Online
View Journal | View Issue

Cite this: *RSC Adv.*, 2020, **10**, 16875

Properties of amorphous iron phosphate in pseudocapacitive sodium ion removal for water desalination

Abdulaziz Bentalib, Yanbo Pan, Libo Yao and Zhenmeng Peng *

Received 2nd March 2020
Accepted 23rd April 2020

DOI: 10.1039/d0ra02010a

rsc.li/rsc-advances

Capacitive deionization (CDI) is an energy saving and environmentally friendly technology for water desalination. However, classical CDI is challenged by a low salt removal capacity. To improve the desalination capacity, electrode materials utilizing the battery mechanism for salt ion removal have emerged as a new direction more recently. In this work, we report a study of amorphous iron phosphate ($FePO_4$) as a promising electrode material for pseudocapacitive sodium ion removal. Sodium ions can be effectively, reversibly intercalated and de-intercalated upon its electrochemical reduction and oxidation, with an excellent sodium ion capacity under half-cell testing conditions. By assembling a hybrid CDI (HCDI) system utilizing the $FePO_4$ electrode for pseudocapacitive sodium ion removal and active carbon electrode for capacitive chloride ion removal, the cell exhibited a high salt removal capacity and good reversibility and durability, which was attributed to the advantageous features of amorphous $FePO_4$. The HCDI system achieved a high deionization capacity (82 mg g^{-1}) in 10 mM NaCl, a fast deionization rate (0.046 mg g^{-1} s^{-1}), and good stability and cyclability.

1. Introduction

The world's population is increasing at a rate that makes fresh water provision an ever-developing challenge. In addition, pollution complicates the available water resources supply. According to research conducted by the United Nations Educational, Scientific and Cultural Organization (UNESCO), there are over two billion individuals now struggling with less than adequate water supply worldwide, and by 2050, nearly five billion will fit into this category (UNESCO, 2019). Because of this international shortage of satisfactory drinking water, there is an urgent demand for safe and efficient desalination technology.[1]

The following techniques exist as the most commonly proposed solutions for providing desalted water: reverse osmosis,[2] multistage flash distillation,[3] and multi-effect distillation.[4] Unfortunately, these methods are energy intensive and costly, especially when used for the desalination of brackish water or sea water—and nearly all available water falls into these two categories—where the concentration of salt is more than 10 000 mg L^{-1}.[5,6]

In contrast, capacitive deionization (CDI) is considered an alternative, much more energy-efficient method for removing salt from water with a low or medium salinity. As CDI is used to desalinate brackish water, it uses a far lower amount of energy (0.13–0.59 kW h m^{-3}) than is used by common reverse osmosis (0.7–2.0 kW h m^{-3}).[7] An additional advantage of CDI is that it does not require the use of either thermal energy input or the complicated membrane module. Instead, the device's performance is determined primarily by the materials in the electrode. In summary, the CDI technique offers multiple benefits: energy conservation, simpler process, lower cost, and sustainability.[8]

The CDI concept was pioneered in the early 1960s.[9] Since the 1995 research by Farmer, *et al.*,[10] reporting the use of carbon aerogel in CDI electrodes, carbon has served as the source of extensive study for their excellent electrical conductivity and chemical stability.[11–13] Traditional activated carbon (AC) results in limited CDI performance, which most connect to its absence of intersecting porous structure and highly productive functionality.[14,15] Recent research has focused on preparing newer carbon nanomaterials based on earlier developed graphene, biomass, and metal–organic frameworks.[16–19] Other research has been actively working to improve desalination capacity through methods of chemical activation, heteroatom doping of carbon nanostructures, and surface modification.[20,21] Yet, all researched electrode materials based on the CDI method have resulted in less than satisfactory capacity improvement.[22,23]

Pasta *et al.*[24] first suggested the concept of a "desalination battery" in 2012, instigating research into discriminatory ion separation, ion-enhanced storage, and lessened co-ion expulsion effect.[25–30] This faradaic process allowed greater exploration into further enhancement of desalination performance. One particular eco-friendly material—amorphous iron phosphate ($FePO_4$) costs less and has been extensively considered in sodium ion battery research because of its superior storage capability.[31–33] Nevertheless, due to limited research into this

Department of Chemical, Biomolecular and Corrosion Engineering, The University of Akron, Akron, Ohio 44325, USA. E-mail: zpeng@uakron.edu

material for water desalination,[34] the properties of amorphous $FePO_4$ under the condition of water desalination are inconclusive and require additional careful study.

In this work, we report a new hybrid CDI (HCDI) system, using amorphous $FePO_4$ on activated carbon fiber for faradaic sodium ion removal and using activated carbon (AC) for capacitive chloride ion removal. The use of activated carbon fiber as $FePO_4$ support allows enhanced electric conductivity and ionic diffusion. During the charging and discharging process, sodium ions are intercalated into and de-intercalated from the lattice of $FePO_4$, respectively. In the meantime, chloride ions are physically, electrostatically adsorbed and released on electric double layers (EDL) of the AC electrode. The HCDI system exhibits a high deionization capacity (82 mg g^{-1}), a fast deionization rate (0.046 mg g^{-1} s^{-1}), and good stability and cyclability, confirming the excellent properties of amorphous $FePO_4$ for water desalination application.

2. Experimental section

• Materials

Commercial amorphous $FePO_4 \cdot 2H_2O$ (>99%) was purchased from Sigma-Aldrich. Carbon support (C, Vulcan®XC-72R) was purchased from Cabot. Isopropanol and *N*-methyl-2-pyrrolidone were from Fisher Scientific. The material was characterized by SEM imaging and EDX mapping that were obtained on a Tescan LYRA3 with a working voltage of 10 kV for SEM and 20 kV for the mapping mode. Transmission electron microscopy (TEM) images were taken using a JEOL JEM-1230 microscope with an accelerating voltage of 120 kV. X-ray diffraction (XRD) patterns were recorded on a Bruker AXS Dimension D8 X-ray diffractometer with Cu Kα radiation source.

• Electrode fabrication

The $FePO_4 \cdot 2H_2O$ electrode used in the HCDI system was fabricated by a slurry mixture of 17 mg $FePO_4 \cdot 2H_2O$, 3 mg carbon black and Nafion (20 μL) in 8 mL solvent (50% deionized water: 50% isopropanol in volume ratio). The slurry was sonicated for 30 min to form a uniform ink. The ink was applied into activated carbon fiber mat that was cut with the dimension of 2 in × 2 in and heated at 70 °C during the process. The activated carbon electrode was fabricated by using carbon black and polyvinylidene difluoride (PVDF) binder in a mass ratio of 9 : 1 (0.2 g : 20 mg) which was dissolved in 10 mL *N*-methyl-2-pyrrolidone (NMP). The slurry was stirred and heated at 80 °C overnight to make a uniform mixture. The mixture was applied into activated carbon fiber mat that was cut with the dimension of 2 in × 2 in and heated at 80 °C during the process. After applying the carbon mixture into the activated carbon fiber mat, it was washed several times with deionized water and dried in vacuum at 80 °C for 12 hours prior to use.

• Electrochemical characterization

Cyclic voltammetry (CV) were conducted using a CHI760D electrochemical workstation (CH Instruments, Inc.) using a three-electrode system in an aqueous 0.1 M NaCl electrolyte. The system consisted of $FePO_4 \cdot 2H_2O$ loaded on a 5 mm glassy carbon electrode as the working electrode, a platinum wire as the counter electrode and an Ag/AgCl reference electrode.

• Desalination experiments

The desalination process was carried out in a batch mode cell that consisted of two parallel $FePO_4$ and AC electrodes that were separated by a non-conductive spacer to avoid short-circuiting. The feed water was 30 mL in volume and contained 2 mM, 5 mM and 10 mM of NaCl, respectively. The concentration change was evaluated by measuring the conductivity using a conductivity meter before and after every charging and discharging process. Under constant voltage operations, 1.2 V and 0 V were applied to the HCDI cell for 30 min for each charging and discharging process, respectively. The salt removal capacity (Γ, mg g^{-1}) was calculated according to the equation below:

$$\Gamma = \frac{(C_0 - C_f) \times V}{m} \quad (1)$$

where C_0 and C_f are the initial and final NaCl salt concentration (expressed in mg L^{-1}), V is the total volume of salt solution (L) and m is the mass of electrode materials (g).

The charge efficiency can be determined by the following equation:

$$\eta = \frac{\Gamma \times m \times F}{M_w \times Q} \times 100\% \quad (2)$$

where F is Faraday's constant (96 485 C mol^{-1}), M_w is the molecular weight of NaCl and Q is the total charge passing through the CDI cell during experiment.

3. Result and discussion

The $FePO_4$ was characterized prior to use. Scanning electron microscopy (SEM) and transmission electron microscopy (TEM) imaging show the sample was in form of nanosized powders and the individual particles were highly porous (Fig. 1a and b). Only broad diffraction peaks were observed on the X-ray diffraction (XRD) pattern, which indicated the material was primarily in an amorphous phase Fig. 1c. The energy-dispersive X-ray (EDX) spectrum indicated that there is no trace of Na^+ in the powder and confirmed the composition of $FePO_4$ Fig. 1d.

The electrochemical properties of $FePO_4$ for sodium ion intercalation and de-intercalation were studied in a three-electrode system consisting of an Ag/AgCl reference electrode and a Pt wire counter electrode, and 0.1 M NaCl aqueous solution as the electrolyte. Fig. 2a shows cyclic voltammetry (CV) curves of the $FePO_4$ electrode being collected at scan rate of 10 mV s^{-1} and 50 mV s^{-1}, respectively. The overall shape of the CV curves was tilted within the potential scan range, revealing the participation of faradaic charge transfers. A pair of redox peaks was observed at around 0.2 V, which was consistent with literature data and can be attributed to Fe^{3+}/Fe^{2+} redox couple in $FePO_4$ as depicted in eqn (3).[35] Na^+ intercalation into and de-intercalation from the lattice associate with the redox process, which enables removal of this salt ion following the battery mechanism. The redox potential falls between the

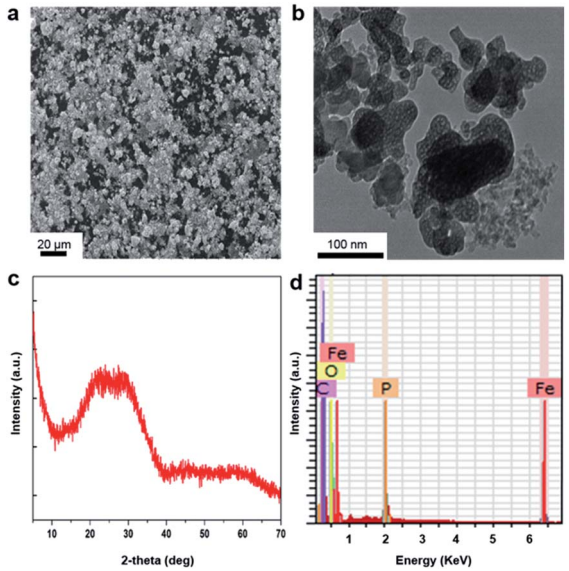

Fig. 1 (a) TEM, (b) SEM, (c) XRD and (d) EDX of $FePO_4$.

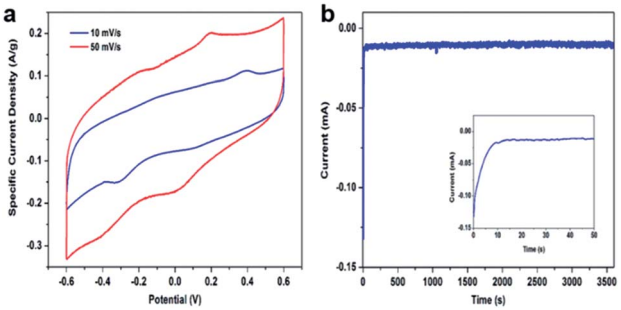

Fig. 2 (a) CV curves of the amorphous $FePO_4$ in 0.1 M NaCl aqueous solution with a scan rate of 50 mV s^{-1} and 10 mV s^{-1}, (b) chronoamperometry at −0.4 V *vs.* Ag/AgCl.

thermodynamic potentials for hydrogen evolution reaction and oxygen evolution reaction (−0.612 V and 0.618 V *vs.* Ag/AgCl at neutral pH). This is a desirable feature for water desalination because it avoids water electrolysis during Na^+ electrochemical intercalation and de-intercalation. A slight decrease in the specific capacity with an increase in the potential scan rate was observed, which was likely due to a more dominance of Na^+ transfer resistance.[36] Fig. 2b shows a chronoamperometry profile collected at −0.4 V, with the cathodic current corresponding to intercalation of Na^+ ions into electrochemically reducing $FePO_4$ lattice. The initial drop in the current value within the first ten seconds can be explained using the capacitive discharging effect. The current decay became significantly more gradual thereafter, indicating a relatively steady cathodic process regulated by the Na^+ ion intercalation rate.

$$FePO_4 + xNa^+ + xe^- \leftrightarrow Na_xFePO_4 \quad (3)$$

Because $FePO_4$ by itself has poor electric conductivity that would cause dramatic internal ohmic loss, $FePO_4$ was loaded

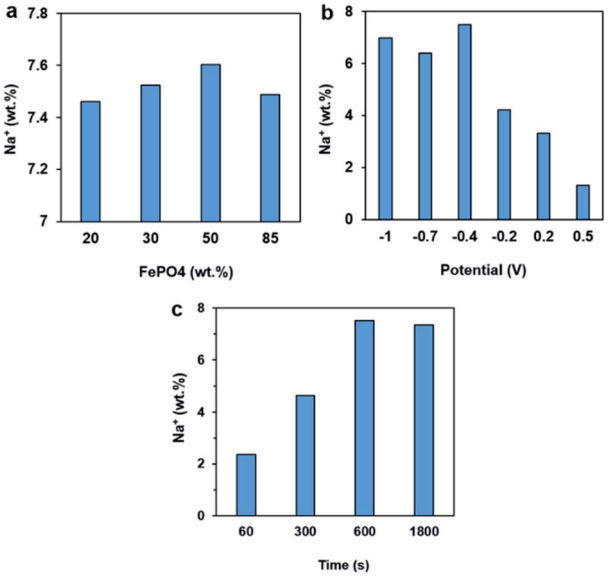

Fig. 3 Effects of (a) $FePO_4$ loading on the carbon support, (b) electrode potential, and (c) time on the Na^+ capacity of amorphous $FePO_4$.

onto carbon support to improve this issue. The formulation effect for preparing $FePO_4$/C electrode materials was examined by adjusting the loading amount and evaluating the Na^+ ion intercalation property, which exhibited only marginal variance in the Na^+ ion storage capacity Fig. 3a. Fig. 3b shows the influence of electrode potential on the Na^+ ion storage capacity, which exhibited an overall trend of a higher capacity being obtained with a more negative potential. The Na^+ ion storage capacity of the $FePO_4$ was also investigated as function of time at −0.4 V Fig. 3c. A merely 2.3 wt% Na^+ capacity was obtained after 60 s of stay at this potential, which continued to increase with time and became nearly doubled after 300 s. The capacity reached a maximum of 7.6 wt% after 600 s of operation. No further increase in the value was achieved with an even longer time, suggesting an equilibrium state. The findings further confirmed the Na^+ ion intercalation process was largely regulated by the lattice atom diffusion, which has slower kinetics than charge transfers.

For evaluating the performance of $FePO_4$ under water desalination condition, a HCDI cell was assembled. As illustrated in Fig. 4, the batch-model cell consisted of $FePO_4$/C loaded on

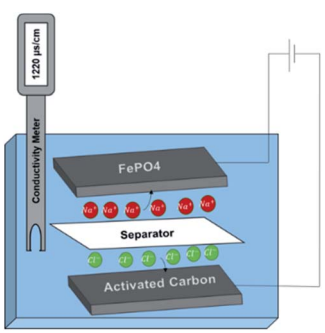

Fig. 4 Scheme of the HCDI system for water desalination experiment.

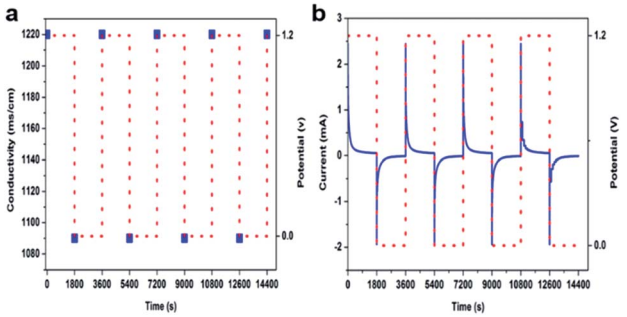

Fig. 5 (a) Salt water conductivity and (b) HCDI current as function of time in response to cell charging at 1.2 V and discharging at 0 V in 30 mL of 10 mM NaCl electrolyte. Blue square represents measured conductivity; dotted line in red represents the charging–discharging procedure; blue line.

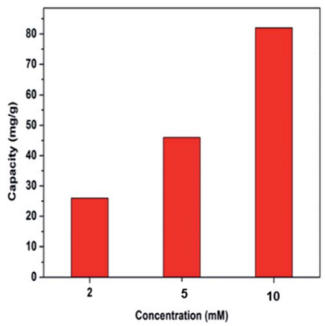

Fig. 6 The desalination capacity determined at different electrolyte concentration.

a carbon cloth as electrode for faradaic Na^+ removal, AC loaded on a carbon cloth as counter electrode for capacitive Cl^- removal, a water-permeable non-conductive separator in between, and aqueous NaCl solution as electrolyte. The two electrodes were connected to a potentiostat for cell voltage control and current measurement. A conductivity meter (TDS, EC, Digital Aid, USA) was used to monitor the water solution conductivity to determine the salt concentration by establishing a calibration curve between the two parameters.

The performance of the assembled HCDI system was evaluated by applying 1.2 V and 0 V cell voltage in the charging and discharging processes, respectively. Fig. 5 show the recorded salt water conductivity and cell current in response to the applied cell voltage. When a 1.2 V voltage was applied, the cell current exhibited an instant drop from 2.49 mA at the very beginning, likely resultant of the CDI effect, which is followed by a more gradual decay over time. The current decreased to 0.05 mA after 1 800 s of operation. During the same time, the salt water conductivity decreased from the initial 1 220 ms cm^{-1} to 1 090 ms cm^{-1}, indicating significant removal of salt ions from the water. After the voltage was switched to 0 V for cell discharging, the conductivity recovered back to about 1 220 ms cm^{-1} within 1 800 s. The recovered value was close to the initial salt water conductivity, suggesting the electrodes are highly reversible. The charging and discharging cycle were repeated for multiple times, with no observable decay in the desalination performance being observed that indicated a good durability of the HCDI system. The charge efficiency of the HCDI, by calculating accumulative charge transfer from Fig. 5b and applying eqn (2), was evaluated to be about 90% for all testing cycles. The value was higher than literature data reported for traditional CDI carbon electrode,[37,38] which can be attributed to the pseudocapacitive property of the amorphous $FePO_4$ which suppresses side faradaic processes.

Fig. 6 compares the deionization capacity of the HCDI system with respect to the NaCl effluent concentration at 2 mM, 5 mM and 10 mM. The desalination capacity values were measured to be 26, 46 and 82 mg g^{-1}, respectively. The finding suggested the HCDI system has an improved performance when desalinating more concentrated salt water. This could be attributed to an improvement of ion transfer inside the electrode pores and a reduction of the electric double layer.[39] Table 1 summarizes some recently reported electrode materials and the properties for comparison. The HCDI system consisting of and active carbon electrodes in this work showed a remarkably high desalination capacity compared with most of other electrodes. The enhanced performance largely benefits from the pseudocapacitive $FePO_4$ electrode which collect and release sodium ions through reversible faradaic intercalation and de-intercalation reactions. Moreover, loading the $FePO_4$ onto the

Table 1 Desalination performance of faradaic electrode based HCDI systems in literature and in this study

Electrode materials	Initial salt concentration	Applied voltage/current density	Deionization capacity (mg g^{-1})	Reference
Cathode: $Na_4Mn_9O_{18}$ anode: activated carbon	10 mM	1.2 V	31.2	20
Cathode: $Na_2FeP_2O_7$ anode: activated carbon	100 mM	1.2 V	30.2	21
Cathode/anode: $Na_2NiFe(CN)_6$	20 mM	2.8 A m^{-2}	34.0	31
Cathode: $Na_{0.44}MnO_2$ anode: AgCl	890 ppm	100 mA g^{-1}	57.4	29
Cathode: $Na_{0.44}MnO_2$ anode: BiOCl	760 ppm	100 mA g^{-1}	68.5	24
Cathode/anode: NaNiHCF	500 mM	5 A m^{-2}	59.9	26
Cathode/anode: MoS_2	400 mM	1.2 V	8.81	24
Cathode/anode: MoS_2 CNT composite	500 mM	0.8 V	25	27
Cathode/anode: Ti_3C_2-MXene	5 mM	1.2 V	13	22
Cathode/anode: hierarchically porous $Ti_3C_2T_x$ MXene aerogel	1000 ppm	1.2 V	45	32
Cathode: $FePO_4$ anode: activated carbon	10 mM	1.2 V	82	This work

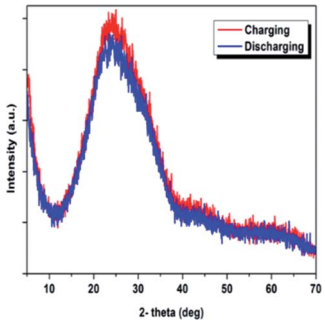

Fig. 7 XRD of the $FePO_4$ electrode (a) after the charging process at 1.2 V and (b) after the discharging process at 0 V.

activated carbon fiber helped to overcome its poor electric conductivity and ionic diffusion. Fig. 7 shows the XRD patterns of the $FePO_4$ after the charging and discharging processes, respectively. No significant changes were observed in the diffractions, suggesting $FePO_4$ remains largely an amorphous structure throughout Na^+ intercalation and de-intercalation reactions.

4. Conclusion

Amorphous $FePO_4$ was studied for the properties in water desalination and exhibited reversible sodium ion intercalation and de-intercalation upon electrochemical reduction and oxidation. The sodium storage capacity was found to reach 7.6 wt% under specific half-cell testing condition. The assembled HCDI system using amorphous $FePO_4$ and active carbon as the two electrodes exhibited a high deionization capacity performance (82 mg g^{-1}) at decent salt removal rate (0.046 mg g^{-1} s^{-1}) compared to many other electrode materials reported in literature. Benefiting from the pseudocapacitive property of the amorphous $FePO_4$, the charge efficiency of the HCDI was improved to 90%. The HCDI also showed good reversibility and durability, evidenced by full recovery of salt water conductivity at completion of a cycle and little capacity decay over operation cycles. The excellent cell performance was attributed largely to the outstanding pseudocapacitive sodium ion removal properties of $FePO_4$. These results suggest amorphous $FePO_4$ as a promising electrode material for sodium ion removal in water desalination.

Conflicts of interest

There are no conflicts of interest to declare.

Acknowledgements

We acknowledge the financial support of this work by National Science Foundation (1665265).

References

1 J. W. Young Jr, *Exploring alternative futures of the World Water System. Building a second generation of World Water Scenarios - Driving force: Climate Change and Variability*, 2010, p. 25.
2 Y. Liu, C. Nie, X. Liu, X. Xu, Z. Sun and L. Pan, Review on carbon-based composite materials for capacitive deionization, *RSC Adv.*, 2015, **5**(20), 15205–15225.
3 R. Semiat, Water Purification: Materials and Technologies, in *Encyclopedia of Materials: Science and Technology*, ed. K. H. J. Buschow, R. W. Cahn, M. C. Flemings, B. Ilschner, E. J. Kramer, S. Mahajan, and P. Veyssière, Elsevier, Oxford, 2010, pp. 1–4.
4 M. A. Anderson, A. L. Cudero and J. Palma, Capacitive deionization as an electrochemical means of saving energy and delivering clean water. Comparison to present desalination practices: will it compete?, *Electrochim. Acta*, 2010, **55**(12), 3845–3856.
5 E. Georgopoulou, A. Kotronarou, A. Koussis, P. J. Restrepo, A. Gómez-Gotor and J. J. Rodriguez Jimenez, A methodology to investigate brackish groundwater desalination coupled with aquifer recharge by treated wastewater as an alternative strategy for water supply in Mediterranean areas, *Desalination*, 2001, **136**(1–3), 307–315.
6 S. Burn, M. Hoang, D. Zarzo, F. Olewniak, E. Campos, B. Bolto and O. Barron, "Desalination techniques — a review of the opportunities for desalination in agriculture, *Desalination*, 2015, **364**, 2–16.
7 S. Porada, R. Zhao, A. van der Wal, V. Presser and P. M. Biesheuvel, Review on the science and technology of water desalination by capacitive deionization, *Prog. Mater. Sci.*, 2013, **58**(8), 1388–1442.
8 C. Zhang, D. He, J. Ma, W. Tang and T. D. Waite, Faradaic reactions in capacitive deionization (CDI) - problems and possibilities: a review, *Water Res.*, 2018, **128**, 314–330.
9 J. W. Blair and G. W. Murphy, *Electrochemical Demineralization of Water with Porous Electrodes of Large Surface Area*, American Chemical Society, 1960, pp. 206–223.
10 J. C. Farmer, D. V. Fix, G. V. Mack, R. W. Pekala and J. F. Poco, Capacitive deionization of NH_4ClO_4 solutions with carbon aerogel electrodes, *J. Appl. Electrochem.*, 1996, **26**(10), 1007–1018.
11 A. C. Power, B. Gorey, S. Chandra and J. Chapman, Carbon nanomaterials and their application to electrochemical sensors: a review, *Nanotechnol. Rev.*, 2018, **7**(1), 19–41.
12 M. E. Suss, S. Porada, X. Sun, P. M. Biesheuvel, J. Yoon and V. Presser, Water desalination *via* capacitive deionization: what is it and what can we expect from it?, *Energy Environ. Sci.*, 2015, **8**(8), 2296–2319.
13 P. Xu, J. E. Drewes, D. Heil and G. Wang, Treatment of brackish produced water using carbon aerogel-based capacitive deionization technology, *Water Res.*, 2008, **42**(10–11), 2605–2617.
14 Z. Huang, Z. Yang, F. Kang and M. Inagaki, Carbon Electrodes for Capacitive Deionization, *J. Mater. Chem. A*, 2017, **5**, 470–496.
15 M. A. Ahmed and S. Tewari, Capacitive deionization: processes, materials and state of the technology, *J. Electroanal. Chem.*, 2018, **813**, 178–192.
16 W. Huang, Y. Zhang, S. Bao and S. Song, Desalination by capacitive deionization with carbon-based materials as electrode: a review, *Surf. Rev. Lett.*, 2013, **20**(6), 1330003.

17 J. Kim, J. Kim, J. H. Kim and H. S. Park, Hierarchically open-porous nitrogen-incorporated carbon polyhedrons derived from metal-organic frameworks for improved CDI performance, *Chem. Eng. J.*, 2019, 122996.

18 W. Shi, C. Ye, X. Xu, X. Liu, M. Ding, W. Liu, X. Cao, J. Shen, H. Y. Yang and C. Gao, High-Performance Membrane Capacitive Deionization Based on Metal-Organic Framework-Derived Hierarchical Carbon Structures, *ACS Omega*, 2018, **3**(8), 8506–8513.

19 G. Quan, L. Chu, X. Han, C. Ding, T. Chen and J. Yan, Facile synthesis of novel hierarchically porous carbon derived from nature biomass for enhanced removal of NaCl, *Water Sci. Technol.*, 2016, **74**(8), 1821–1831.

20 O. Barbieri, M. Hahn, A. Herzog and R. Kötz, Capacitance limits of high surface area activated carbons for double layer capacitors, *Carbon*, 2005, **43**(6), 1303–1310.

21 Y. Liu, X. Xu, M. Wang, T. Lu, Z. Sun and L. Pan, Metal-organic framework-derived porous carbon polyhedra for highly efficient capacitive deionization, *Chem. Commun.*, 2015, **51**(60), 12020–12023.

22 B. Han, G. Cheng, Y. Wang and X. Wang, Structure and functionality design of novel carbon and faradaic electrode materials for high-performance capacitive deionization, *Chem. Eng. J.*, 2019, **360**, 364–384.

23 E. Avraham, M. Noked, Y. Bouhadana, A. Soffer and D. Aurbach, Limitations of charge efficiency in capacitive deionization processes III: the behavior of surface oxidized activated carbon electrodes, *Electrochim. Acta*, 2010, **56**(1), 441–447.

24 M. Pasta, C. D. Wessells, Y. Cui and F. La Mantia, A desalination battery, *Nano Lett.*, 2012, **12**(2), 839–843.

25 J. Lee, S. Kim, C. Kim and J. Yoon, Hybrid capacitive deionization to enhance the desalination performance of capacitive techniques, *Energy Environ. Sci.*, 2014, **7**(11), 3683–3689.

26 S. Kim, J. Lee, C. Kim and J. Yoon, $Na_2FeP_2O_7$ as a Novel Material for Hybrid Capacitive Deionization, *Electrochim. Acta*, 2016, **203**, 265–271.

27 T. Chen, J. Meng, S. Wu, J. Pei, Q. Lin, X. Wei, J. Li and Z. Zhang, Room temperature synthesized $BaTiO_3$ for photocatalytic hydrogen evolution, *J. Alloys Compd.*, 2018, **754**, 184–189.

28 H. Yin, S. Zhao, J. Wan, H. Tang, L. Chang, L. He, H. Zhao, Y. Gao and Z. Tang, Three-dimensional graphene/metal oxide nanoparticle hybrids for high-performance capacitive deionization of saline water, *Adv. Mater.*, 2013, **25**(43), 6270–6276.

29 J. Cao, Y. Wang, L. Wang, F. Yu and J. Ma, $Na_3V_2(PO_4)_3$ @C as Faradaic Electrodes in Capacitive Deionization for High-Performance Desalination, *Nano Lett.*, 2019, **19**(2), 823–828.

30 W. Zhao, M. Ding, L. Guo and H. Y. Yang, Dual-Ion Electrochemical Deionization System with Binder-Free Aerogel Electrodes, *Small*, 2019, **15**(9), 1–8.

31 Y. Wang, Z. Feng, D. Laul, W. Zhu, M. Provencher, M. L. Trudeau, A. Guerfi and K. Zaghib, Ultra-low cost and highly stable hydrated $FePO_4$ anodes for aqueous sodium-ion battery, *J. Power Sources*, 2018, **374**, 211–216.

32 G. Yang, B. Ding, J. Wang, P. Nie, H. Dou and X. Zhang, Excellent cycling stability and superior rate capability of a graphene-amorphous $FePO_4$ porous nanowire hybrid as a cathode material for sodium ion batteries, *Nanoscale*, 2016, **8**(16), 8495–8499.

33 Z. C. Shi, A. Attia, W. L. Ye, Q. Wang, Y. X. Li and Y. Yang, Synthesis, characterization and electrochemical performance of mesoporous $FePO_4$ as cathode material for rechargeable lithium batteries, *Electrochim. Acta*, 2008, **53**(6), 2665–2673.

34 J. Ma, L. Wang, F. Yu and X. Dai, Mesoporous amorphous $FePO_4$ nanosphere@graphene as a faradic electrode in capacitive deionization for high-capacity and fast removal of NaCl from water, *Chem. Eng. J.*, 2019, **370**, 938–943.

35 L. Wu and D. W. Shoesmith, An electrochemical study of H_2O_2 oxidation and decomposition on simulated nuclear fuel (SIMFUEL), *Electrochim. Acta*, 2014, **137**, 83–90.

36 B. Talluri, S. Ghosh, G. R. Rao and T. Thomas, Nanocomposites of digestively ripened copper oxide quantum dots and graphene oxide as a binder free battery-like supercapacitor electrode material, *Electrochim. Acta*, Oct. 2019, **321**, 134709.

37 P. M. Biesheuvel and A. van der Wal, Membrane capacitive deionization, *J. Membr. Sci.*, 2010, **346**(2), 256–262, DOI: 10.1016/j.memsci.2009.09.043.

38 B. H. Min, J. H. Choi and K. Y. Jung, Improved capacitive deionization of sulfonated carbon/titania hybrid electrode, *Electrochim. Acta*, 2018, **270**, 543–551, DOI: 10.1016/j.electacta.2018.03.079.

39 S. Tian, Z. Zhang, X. Zhang and K. Ostrikov, Capacitative deionization using commercial activated carbon fiber decorated with polyaniline, *J. Colloid Interface Sci.*, 2019, **537**, 247–255.

